

# A CP-free STBC-MIMO OFDM communication system with ISI suppression capability for underwater multipath channel

Shiho Oshiro  
Graduate School of Engineering  
and Science  
University of the Ryukyus  
Okinawa, Japan  
[k208674@ie.u-ryukyu.ac.jp](mailto:k208674@ie.u-ryukyu.ac.jp)

Hiromasa Yamada  
Oki Seatec Co., Ltd  
Shizuoka Japan  
[yamada882@oki.com](mailto:yamada882@oki.com)

Shigeo Nakagawa  
Cyohemon GK  
Shizuoka Japan  
[naka@cyoh.co.jp](mailto:naka@cyoh.co.jp)

Tomohisa Wada  
Dept. of Engineering  
University of the Ryukyus  
Okinawa, Japan  
[wada@ie.u-ryukyu.ac.jp](mailto:wada@ie.u-ryukyu.ac.jp)

**Abstract**—Because of a progress in marine development for seabed natural resource, deep sea exploring becomes essential. Then, wireless underwater communication has become important to communicate with distanced terminals. In case that the signal propagation channel contains reflection objects such as sea surface and structures in the sea, plural delayed signals are generated and cause the Inter Symbol Interference (ISI) between transmitting symbols. To avoid the ISI degradation, acoustic OFDM communication system inserts gap interval between successive OFDM symbols such as Cyclic Prefix (CP). However, the insertion of CP lowers data transmission bandwidth.

This study evaluates an ISI suppression performance for underwater communication system using Space Time Block Code (STBC) with MIMO OFDM system [1-2] with no CP insertion. Previously we have reported computer simulation results as [3], and this paper describes improved signal processing method and Ocean experiment results.

Simulated Bit Error Rate (BER) performance vs maximum Multipath Delay  $L$ . Multipath condition is one direct wave and additional  $L$  delayed waves with linearly degraded amplitude and random phase. In case of SNR (dB) more than 20 dB, 70 points delay (corresponding to 11 ms) for 128 points OFDM symbol (20ms length) is successfully suppressed, which corresponds to 55% ISI condition.

We used two transmitting and 4 receiving transducers. The distance between TX and RX is roughly 6.0m. 3.3 ms multipath delay is observed with 20ms OFDM symbol. Which corresponds to 16.5% Inter-Symbol-Interference (ISI) condition. Measured constellations for simple OFDM with no CP and 2x4 STBC-MIMO OFDM with no CP. And corresponding measured BERs are 0.0401 and 0.0023, respectively. Because of ISI, the OFDM with no CP suffers the ISI and the BER is degraded, while CP-free 2x4 STBC-MIMO OFDM has shown improved BER because of ISI suppression capability. In this simulation, time series distortion was observed. For time series distortion, BER was improved when AIF canceled. And corresponding measured BER is 0.0017. the BER of CP-free STBC-MIMO OFDM (AIF can cell), which we used to deal with distortion, was the smallest.

**Keywords**—component, formatting, style, styling, insert (key words)

## I. INTRODUCTION

Because of a progress in marine development for seabed natural resources such as hydrothermal deposits, methane hydrates, deep sea exploring becomes essential. Especially, AUV (autonomous underwater vehicle) without any wires is demanded since its searching area is not restricted by wire length. Then, wireless underwater communication has been become important to acquire AUV collected data without docking. Fig.1 shows a target application of the STBC-MIMO communication system. Since the signal propagation direction is horizontal, delayed signal is caused by reflection at the surface and bottom of the sea. By enabling high bandwidth wireless communication between AUV and base station, AUV can continue a deep seabed exploring without rendezvousing with the station.

In this paper, we propose an underwater acoustic STBC-MIMO OFDM communication system without cyclic prefix based on the algorithm in the papers [1-2]. Fig.2 shows the block diagram of STBC-MIMO OFDM system. The transmitter side has two elements while the receiver side equips more than 3 elements. At the transmitter side, Alamouti's code is used [3]. At the receiver side, STBC decode is performed with compensation of both Inter Symbol Interference (ISI) and Inter Carrier

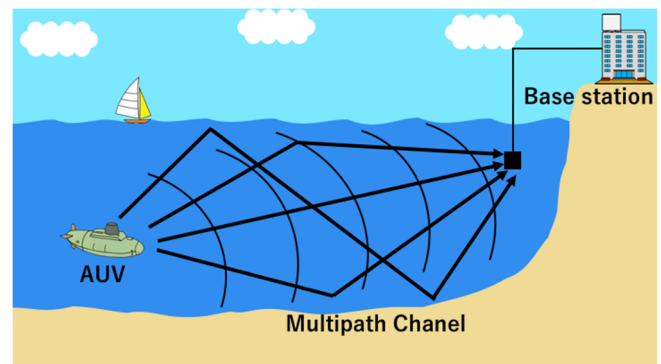


Fig. 1: Target application of STBC-MIMO communication system.

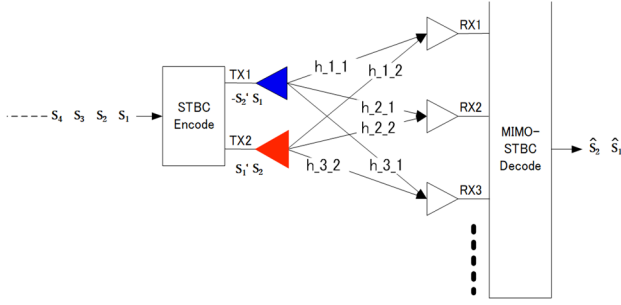


Fig. 2: Block Diagram of conventional STBC-MIMO communication system.

Interference (ICI) by heavy signal processing. In the paper we posted earlier, we compared STBC-MIMO OFDM with and without CP. However, as we went on with my research, we thought that using Oblique Projection (OB) would have better performance.

In the section II, at first conventional OFDM system with CP is shown. Then the proposed STBC-MIMO system architecture will be disclosed. The detail of the ISI and ICI compensation are also described. And we propose STBC-MIMO OFDM system with Oblique Projection. The section III shows computer simulated result of comparison between OFDM with CP and other CP-free STBC-MIMO OFDM. The section Finally, the summary is concluded in section IV.

## II. SYSTEM ARCHITECTURE

### A. STBC-MIMO OFDM system with CP

Fig. 3 shows a block diagram of a conventional OFDM communication system. The upper side corresponds to transmitter and the lower side is receiver. First, bit information is modulated by PSK/QAM mapper. Then the mapped outputs are serial to parallel (S/P) converted to make N-symbols packet. The N-symbols frequency domain packet is IFFTed to make N-points time domain baseband OFDM symbol. As shown in yellow box, the tail parts are copied to the head as Cyclic Prefix (CP) addition. The purpose of CP is to remove ISI from the time delayed previous OFDM symbol to current OFDM symbol as far as the delay is smaller than CP length. In the receiver side, reverse operation is performed. However, since multi-path transmission channel causes signal distortion, the Equalization process is applied for the FFT outputs in the receiver. To perform the equalization, transmission channel estimation

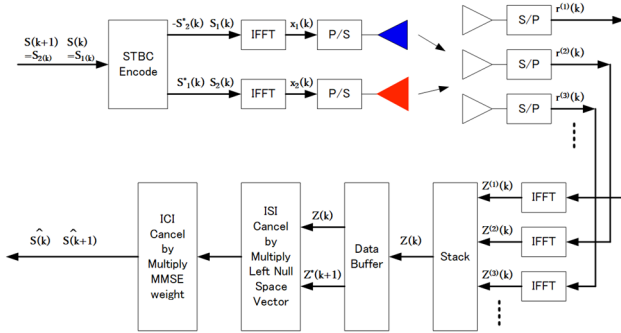


Fig. 3: Block diagram of CP free STBC-MIMO OFDM system.

Identify applicable funding agency here. If none, delete this text box.

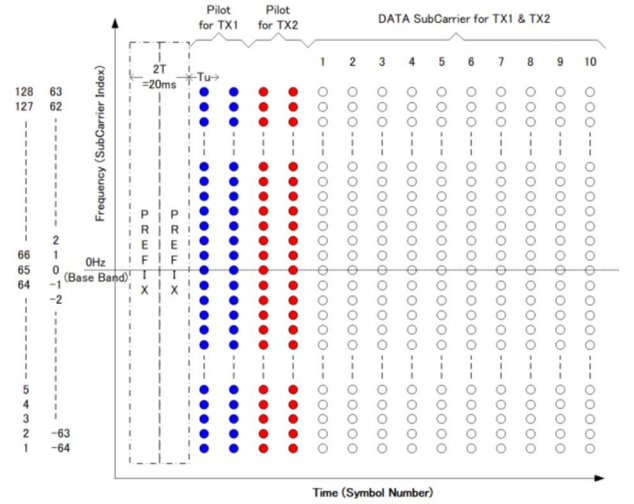


Fig. 4: The blue SPs are only for TX1 element and red SPs are only for TX2 element. The SPs are used for channel estimation.

(Channel Impulse Response or Channel Transfer Function estimation) is required but it is not included.

### B. CP-free STBC-MIMO OFDM system

Fig. 3 shows CP free STBC-MIMO OFDM system. The  $S_1(k)$ ,  $S_2(k)$  are PSK/QAM modulated signal packets similar to the conventional OFDM. By STBC Alamouti's encoding, two time slots, two OFDM symbols are generated by two parallel IFFTs. Let  $s(k)$  and  $s(k+1)$  be two N-dimensional M-ary QAM transmitted symbol blocks. After STBC encoder, It is equation (1) that the transmitted data sequence. Equation (2) is the time domain OFDM symbol block to be send from the ith transmit antenna. At 1st time slot,  $S_1(k)$ ,  $S_2(k)$  are IFFTed to generate  $x_1(k)$ ,  $x_2(k)$  vectors. Then at 2nd time slot,  $-S_2^*(k)$ ,  $S_1^*(k)$  are IFFTed to generate  $x_1(k+1)$ ,  $x_2(k+1)$  vectors.  $S_1^*(k)$  is complex conjugate of  $S_1(k)$ . Those two time slots are pairs for STBC encoding and decoding.

$$\dots \begin{bmatrix} -s_2^*(k) \\ s_1^*(k) \end{bmatrix} \begin{bmatrix} s_1(k) \\ s_2(k) \end{bmatrix} \begin{bmatrix} -s_2^*(k-1) \\ s_1^*(k-1) \end{bmatrix} \begin{bmatrix} s_1(k-1) \\ s_2(k-1) \end{bmatrix} \dots \quad \cdot \cdot \cdot (1)$$

$$x_i(k) = F^H s_i(k), \quad 1 \leq i \leq 2 \quad \cdot \cdot \cdot (2)$$

Fig. 4 shows time-frequency representation of the STBC-MIMO OFDM signals. The used FFT/IFFT size is 128. Then each vertical line of circles are corresponds to one OFDM symbol. To perform channel estimation Scattered Pilot (SP) symbols are inserted. The blue subcarriers are only for blue transmit element (TX1) and the red subcarriers are for red transmit element (TX2) as shown in Fig. 4. The white circles corresponds to modulated symbol such as  $S_1(k)$ ,  $S_2(k)$ . The auxiliary matrices  $H_0(k)$ ,  $H_1(k-1)$  and  $n(k)$  are general referred. Equation (4) is the time  $k+1$ .

$$r(k) = \begin{bmatrix} H_0^{(1,1)}(k) & H_0^{(1,2)}(k) \\ \vdots & \vdots \\ H_0^{(M,1)}(k) & H_0^{(M,2)}(k) \end{bmatrix} F_2^H \begin{bmatrix} s_1(k) \\ s_2(k) \end{bmatrix} + \begin{bmatrix} H_1^{(1,1)}(k-1) & H_1^{(1,2)}(k-1) \\ \vdots & \vdots \\ H_1^{(M,1)}(k-1) & H_1^{(M,2)}(k-1) \end{bmatrix} F_2^H \begin{bmatrix} -s_2^*(k-1) \\ s_1^*(k-1) \end{bmatrix}$$

$$+ \begin{bmatrix} n^{(1)}(k) \\ \vdots \\ n^{(M)}(k) \end{bmatrix} \cdot \cdot \cdot (4)$$

The multichannel system model can be described in terms of signal subspace  $\langle H_0(k) \rangle$ , structured noise subspace  $\langle H_1(k-1) \rangle$  and unstructured noise vector  $n(k)$ . The channel matrix  $H_1(k-1)$  models the overall effect of Inter Symbol Interference (ISI), from the previous to the current block, while  $H_0(k)$  models the overall Inter Carrier Interference (ICI) effect.  $P_{H_L(k-1)}^\perp$  be denoted as orthogonal projection complement of  $H_L(k-1)$ , Insert  $P_{H_L(k-1)}^\perp$  into equation (3).

$$P_{H_L(k-1)}^\perp r(k) = P_{H_L(k-1)}^\perp F_2^H \begin{bmatrix} s_1(k) \\ s_2(k) \end{bmatrix} + P_{H_L(k-1)}^\perp n(k) \cdot \cdot \cdot (5)$$

Equation (5) can be express by the solution of least squares.

$$P_{H_L(k-1)}^\perp r(k) \approx P_{H_L(k-1)}^\perp H_0(k) F_2^H \begin{bmatrix} \hat{s}_1(k) \\ \hat{s}_2(k) \end{bmatrix} \cdot \cdot \cdot (6)$$

According to the normal equation, we can express equation (5) as

$$\begin{aligned} & \left( P_{H_L(k-1)}^\perp H_0(k) \right)^H P_{H_L(k-1)}^\perp r(k) = \\ & \left( P_{H_L(k-1)}^\perp H_0(k) \right)^H P_{H_L(k-1)}^\perp H_0(k) F_2^H \begin{bmatrix} \hat{s}_1(k) \\ \hat{s}_2(k) \end{bmatrix} \cdot \cdot \cdot (7) \end{aligned}$$

We obtain the least-squares estimate of the desired OFDM signal.

$$\begin{aligned} & \left( \left( P_{H_L(k-1)}^\perp H_0(k) \right)^H P_{H_L(k-1)}^\perp H_0(k) \right)^{-1} \left( P_{H_L(k-1)}^\perp H_0(k) \right)^H P_{H_L(k-1)}^\perp r(k) \\ & = F_2^H \begin{bmatrix} \hat{s}_1(k) \\ \hat{s}_2(k) \end{bmatrix} \cdot \cdot \cdot (8) \end{aligned}$$

Since the orthogonal projection matrix  $P_{H_L(k-1)}^\perp$  have a property as  $P_{H_L(k-1)}^\perp P_{H_L(k-1)}^\perp = P_{H_L(k-1)}^\perp$ , this equation(8) can be rewritten as

$$\begin{aligned} & \left( H_0^H(k) P_{H_L(k-1)}^\perp H_0(k) \right)^{-1} H_0^H(k) P_{H_L(k-1)}^\perp r(k) \\ & = F_2^H \begin{bmatrix} \hat{s}_1(k) \\ \hat{s}_2(k) \end{bmatrix} \cdot \cdot \cdot (9) \end{aligned}$$

Table 1: System Parameters

Parameters	Value
TX-RX Elements	2TX and 4 RX 2x4 STBC MIMO
Sampling Frequency	6.4k Hz
TX Center Frequency	16k Hz
Band Width	6.4k Hz
FFT Size	128
OFDM symbol length T	20.0 ms (128 points)
CP length T <sub>cp</sub>	0ms, CP free
Sub-Carrier Spacing	50.0 Hz
Number of Sub Carrier	128
Channel Estimation	Two Symbols for each TX1 and TX2
Modulation	QPSK/16QAM

We may per

multiply the channel signature matrix,  $H_0(k)$ , on both sides of equation (9), to give equation (10).

$$\begin{aligned} & H_0(k) \left( H_0^H(k) P_{H_L(k-1)}^\perp H_0(k) \right)^{-1} H_0^H(k) P_{H_L(k-1)}^\perp r(k) \\ & = H_0(k) F_2^H \begin{bmatrix} \hat{s}_1(k) \\ \hat{s}_2(k) \end{bmatrix} \cdot \cdot \cdot (10) \end{aligned}$$

$$\begin{aligned} & E_{H_0(k-1)H_L(k-1)} = H_0(k) \left( H_0^H(k) P_{H_L(k-1)}^\perp H_0(k) \right)^{-1} \\ & \times H_0^H(k) P_{H_L(k-1)}^\perp \cdot \cdot \cdot (11) \end{aligned}$$

The ISI free data only belong to the subspace  $\langle H_0(k) \rangle$ , after projection operator.

$$E_{H_0(k)H_L(k-1)} r(k) \subseteq \langle H_0(k) \rangle \cdot \cdot \cdot (12)$$

Equation (13) is obtained for time  $k+1$ .

$$\begin{aligned} & E_{H_0(k+1)H_L(k)} = H_0(k+1) \left( H_0^H(k+1) P_{H_L(k)}^\perp H_0(k+1) \right)^{-1} \\ & \times H_0^H(k+1) P_{H_L(k)}^\perp \cdot \cdot \cdot (13) \end{aligned}$$

The QR decomposition with Householder transformation is shown in Equation 14.

$$\begin{aligned} & E_{H_0(k)H_L(k-1)} \\ & = Q_{H_0(k)_1} \left( Q_{H_L(k-1)_2}^H Q_{H_0(k)_1} \right)^\dagger Q_{H_L(k-1)_2}^H \cdot \cdot \cdot (14) \end{aligned}$$

We may indicate the pseudo-inverse,  $A^\dagger = (A^H A)^{-1} A^H$ . The time  $k+1$  show in equation (15).

$$\begin{aligned} & E_{H_0(k+1)H_L(k)} \\ & = Q_{H_0(k+1)_1} \left( Q_{H_L(k)_2}^H Q_{H_0(k+1)_1} \right)^\dagger Q_{H_L(k)_2}^H \cdot \cdot \cdot (15) \end{aligned}$$

### C. STBC-MIMO OFDM system with Oblique Projection

Figure 5 shows an STBC-MIMO OFDM system with Oblique Projection. Equation (3) is preprocessed with the QR-based Oblique Projection(OB) operator  $E_{H_0(k)H_L(k-1)}$ , defined in equation(14), such that the structured noise is completely removed, while signal model matrix  $H_0(k)$  is remained undisturbed,

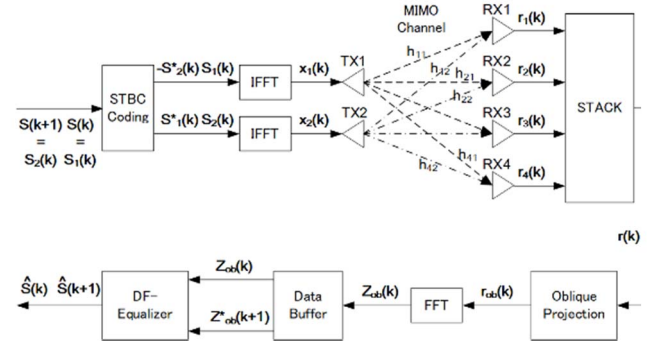


Fig. 5: This is STBC-MIMO OFDM system with Oblique Projection. The blue SPs are only for TX1 element and red SPs are only for TX2 element. The SPs are used for channel estimation.

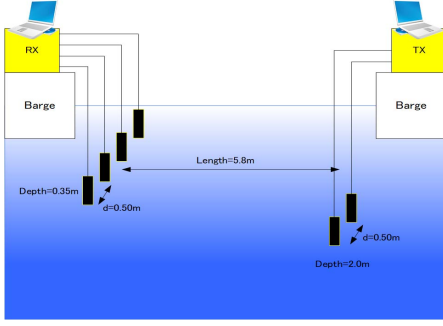


Fig. 6: The figure is structure of ocean experiment.

$$\begin{aligned} r_{ob}(k) &= E_{H_0(k)H_1(k-1)}r(k) \\ &= H_0(k)F_2^H \begin{bmatrix} s_1(k) \\ s_2(k) \end{bmatrix} + E_{H_0(k)H_1(k-1)}n(k) \quad \dots (16) \end{aligned}$$

The structure of matrix  $H_0^{(m,i)}(k)$  and  $H_1^{(m,i)}(k-1)$  as show in equation (17) and equation (18), has a property that the  $N \times N$  matrix  $H_0^{(m,i)}(k) + H_1^{(m,i)}(k-1)$ , a circulant matrix. According to the definition of matrices  $H_0(k)$  and  $H_1(k)$  in equation (3), we can rewrite the equation (19)

$$H_0^{(m,i)}(k) = \begin{pmatrix} h_0^{(m,i)}(k) & 0 & \dots & 0 & \dots & 0 \\ \vdots & \vdots & \ddots & \vdots & \ddots & \vdots \\ h_L^{(m,i)}(k) & \vdots & \vdots & 0 & \vdots & 0 \\ 0 & \vdots & \vdots & h_0^{(m,i)}(k) & \vdots & 0 \\ \vdots & \vdots & \vdots & \vdots & \ddots & \vdots \\ 0 & \dots & 0 & h_L^{(m,i)}(k) & \dots & h_0^{(m,i)}(k) \end{pmatrix} \dots (17)$$

$$H_1^{(m,i)}(k-1) = \begin{pmatrix} 0 & \dots & 0 & h_L^{(m,i)}(k-1) & \dots & h_1^{(m,i)}(k-1) \\ \vdots & \vdots & \vdots & \vdots & \ddots & \vdots \\ 0 & \vdots & \vdots & 0 & \vdots & h_L^{(m,i)}(k-1) \\ \vdots & \vdots & \vdots & \vdots & \ddots & \vdots \\ 0 & \dots & 0 & 0 & \dots & 0 \end{pmatrix} \dots (18)$$

$$\begin{aligned} r_{ob}(k) &= (H_0(k) + H_1(k))F_2^H \begin{bmatrix} s_1(k) \\ s_2(k) \end{bmatrix} \\ &\quad - H_1(k)F_2^H \begin{bmatrix} s_1(k) \\ s_2(k) \end{bmatrix} + E_{H_0(k)H_1(k-1)}n(k) \quad \dots (19) \end{aligned}$$

After demodulation by FFT matrix the frequency domain multiple received signals in equation (20).

$$\begin{aligned} z_{ob}(k) &= F_M r_{ob}(k) = F_M (H_0(k) + H_1(k))F_2^H \begin{bmatrix} s_1(k) \\ s_2(k) \end{bmatrix} \\ &\quad - F_M H_1 F_2^H \begin{bmatrix} s_1(k) \\ s_2(k) \end{bmatrix} + F_M E_{H_0(k)H_1(k-1)}n(k) \quad \dots (20) \end{aligned}$$

Frequency-domain representation equation (A) and (B) will be combined for STBC decoder, which can be expressed in a vector-matrix form equation(21).

$$\begin{aligned} \begin{bmatrix} z_{ob}(k) \\ z_{ob}^*(k+1) \end{bmatrix} &= \begin{bmatrix} D(k) \\ D^*(k+1)J \end{bmatrix} \begin{bmatrix} s_1(k) \\ s_2(k) \end{bmatrix} - \begin{bmatrix} F_M H_1 F_2^H \\ F_M^* H_1^*(k+1) F_2^T J \end{bmatrix} \begin{bmatrix} s_1(k) \\ s_2(k) \end{bmatrix} \\ &\quad + \begin{bmatrix} v(k) \\ v^*(k+1) \end{bmatrix} \quad \dots (21) \end{aligned}$$

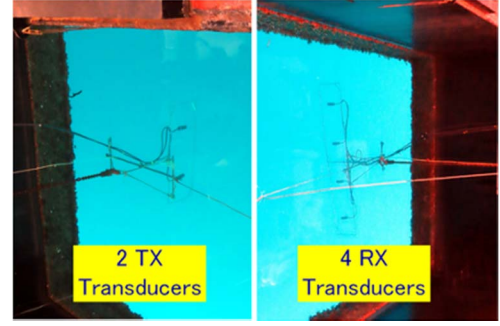


Fig. 7: A photo of two transmitting and 4 receiving transducers.

The ISI-free data model is reduced to equation (22). We can delete ICI by using  $\Gamma^H(k+1) \begin{bmatrix} D(k) \\ D^*(k+1)J \end{bmatrix}$ .

$$\begin{aligned} \bar{z}(k+1) &= \Gamma^H(k+1) \begin{bmatrix} z_{ob}(k) \\ z_{ob}^*(k+1) \end{bmatrix} \\ &= \Gamma^H(k+1) \begin{bmatrix} D(k) \\ D^*(k+1)J \end{bmatrix} \begin{bmatrix} s_1(k) \\ s_2(k) \end{bmatrix} \\ &\quad + \Gamma^H(k+1) \begin{bmatrix} v(k) \\ v^*(k+1) \end{bmatrix} \quad \dots (22) \end{aligned}$$

In the following section, 4 element receiver cases are examined by computer simulation program Matlab.

Summary of the STBC-MIMO OFDM system feature is shown in Table I. OFDM symbol length T is 20.0 ms, which corresponds to 128 sampling points and subcarrier spacing is 50.0 Hz. Carrier Modulation is QPSK and 16QAM.

### III. COMPUTER SIMULATION

The ocean experiment was performed in Barge moon pool with 30m depth at Uchiura bay, Numazu Japan. Fig. 6 is structure of ocean experiment. Fig. 7 shows a photo of two transmitting and 4 receiving transducers. The distance between TX and RX is roughly 6.0 m. Measured delay profile is shown in Fig. 8. 3.3 ms multipath delay is observed with 20ms OFDM symbol. Which corresponds to 16.5% Inter-Symbol-Interference (ISI) condition. Measured constellations for simple OFDM with no CP and 2x4 STBC-MIMO OFDM with no CP are shown as Figs 9a and 9b. And corresponding measured BERs are 0.0401 and 0.0023, respectively. Because of ISI, the OFDM with no CP suffers

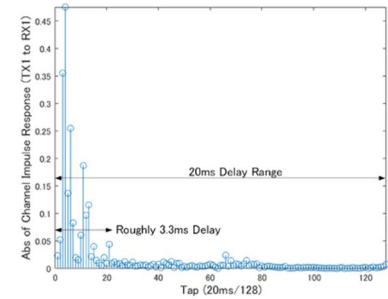


Fig. 8: Measured Delay Profile at Ocean Barge experiment shown in Fig7. 3.3ms multipath delay is observed with 20ms OFDM symbol. 16.5% Inter-Symbol-Interference (ISI) condition.

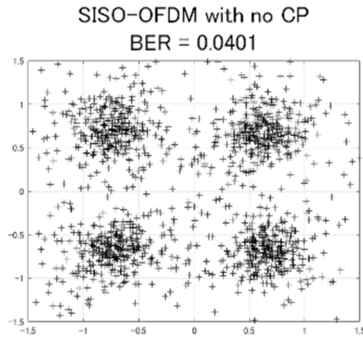


Fig. 9a: Measured QPSK Constellation with 1x1 SISO OFDM. Because of ISI, degraded BER of 0.0401 is observed.

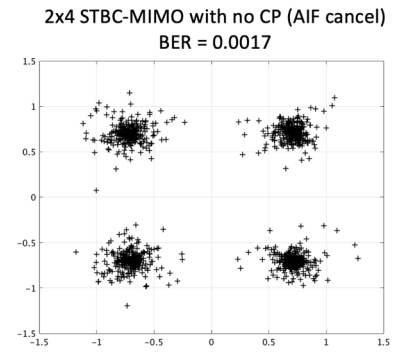


Fig. 11: Measured QPSK Constellation with 2x4 STBC- MIMO OFDM Improved BER of 0.0017 is observed by AIF cancel.

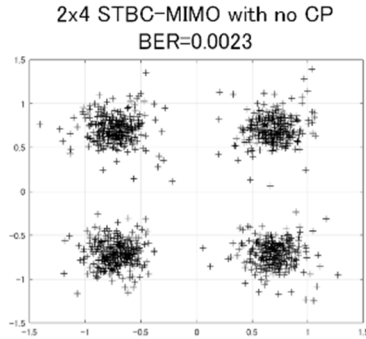


Fig. 9b: Measured QPSK Constellation with 2x4 STBC- MIMO OFDM. Improved BER of 0.0023 is observed by ISI suppression capability.

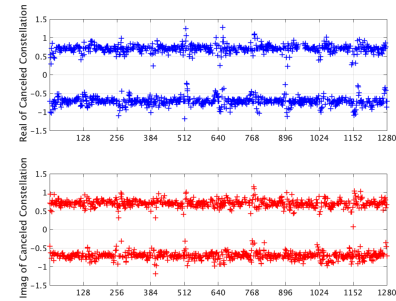


Fig. 12: This figure is canceled constellation after AIF cancel

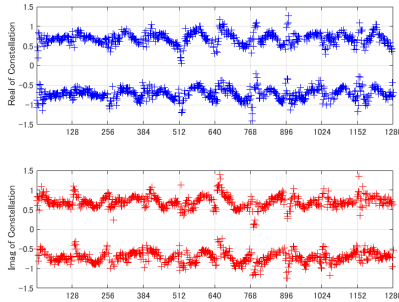


Fig. 10: This figure is time series distortion was observed.

the ISI and the BER is degraded, while CP-free 2x4 STBC-MIMO OFDM has shown improved BER because of ISI suppression capability.

In this simulation, time series distortion was observed as shown in Fig. 10. Based on this result, BER improved when AIF was canceled as shown in Fig. 11. After AIF cancel, we can cancel distorted time series distortion as shown in Fig. 12. And corresponding measured BER is 0.0017. Figure 13 is a result of comparison between CP-free OFDM, OFDM with CP-free STBC-MIMO OFDM, CP-free STBC MIMO OFDM (AIF cancel). CP-free OFDM has a very high BER because ISI cannot be taken. However, the BER of CP-free STBC-

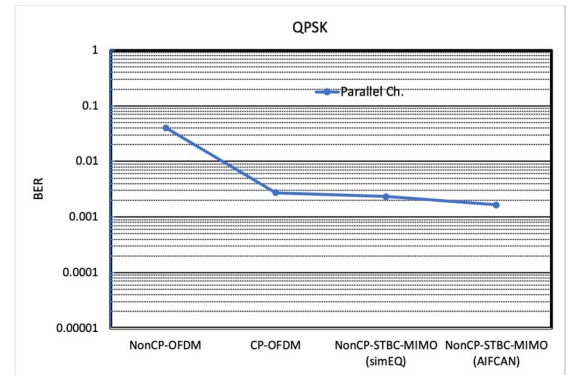


Fig. 13: This graph is a result of comparison between CP-free OFDM, OFDM with CP-free STBC-MIMO OFDM, CP-free STBC MIMO OFDM (AIF cancel).

MIMO OFDM (AIF cancel), which we used to deal with distortion, was the smallest.

#### IV. CONCLUSION

We propose an A CP-free STBC-MIMO OFDM communication system with ISI suppression capability for underwater multipath channel based on the algorithm in the papers [1-2]. The transmitter side has two elements while the receiver side equips more than 4 elements. At the receiver side, STBC decode is performed with compensation of Inter Symbol Interference (ISI) by Oblique Projection. 3.3 ms multipath delay is observed with 20ms OFDM symbol. Which corresponds to 16.5% Inter-Symbol-Interference (ISI) condition. Measured constellations for simple OFDM with no

CP and 2x4 STBC- MIMO OFDM with no CP are shown as figs 6a and 6b. And corresponding measured BERs are 0.0401 and 0.0023, respectively. Because of ISI, the OFDM with no CP suffers the ISI and the BER is degraded, while CP-free 2x4 STBC- MIMO OFDM has shown improved BER because of ISI suppression capability. In this simulation, time series distortion was observed. For time series distortion, BER was improved when AIF canceled. And corresponding measured BER is 0.0017. Result of comparison between CP-free OFDM, OFDM with CP-free STBC-MIMO OFDM, CP-free STBC MIMO OFDM (AIF cancel). CP-free OFDM has a very high BER because ISI cannot be taken. However, the BER of CP-free STBC-MIMO OFDM (AIF can cell), which we used to deal with distortion, was the smallest.

#### REFERENCES

- [1] Chih-Yuan LIN, Jwo-Yuh WU, Ta-Sung LEE, "A Near- Optimal Low-Complexity Transceiver for CP-Free Multi- Antenna OFDM Systems," IEICE Trans. Commun., Vol. E89-B, No.1, January 2006.
- [2] Chih-Wei Wu, Shiunn-Jang Chern, "Novel Frequency Domain DFE with Oblique Projection for CP Free ST-BC MIMO OFDM System," Master Thesis at National Sun Yat- sen University, June 2009.
- [3] Shiho Oshiro, Tomohisa Wada, "A CP-free STBC- MIMO OFDM communication system for underwater multipath channel," IEEE UPCON 2018, MMMUT Gorakhpur, UP India, November 2-4th 2018.
- [4] S.M. Alamouti, "A simple transmit diversity technique for wireless communications," IEEE Journal on Selected Areas in Communications. 16 (8): 1451-1458, October 1998.